Supporting Information

Deciphering the electrochemical kinetics of sulfur vacancy assisted nitrogen doped $NiCo_2S_4$ combined with sulfur doped g-C_3N_4 towards supercapacitor applications

Soumyashree Pany[a], Amtul Nashim[a#], Ritik Mohanty[a#], Kulamani Parida[a]

[a]Centre for Nano Science and Nano Technology, Institute of Technical Education and Research, Siksha 'O' Anusandhan (Deemed to be University), Bhubaneswar, 751030, India,

# Equal Contribution

*Kulamani Parida, *SOA University, Bhubaneswar*-751019,
E-mail: paridakulamani@yahoo.com, kulamaniparida@soa.ac.in

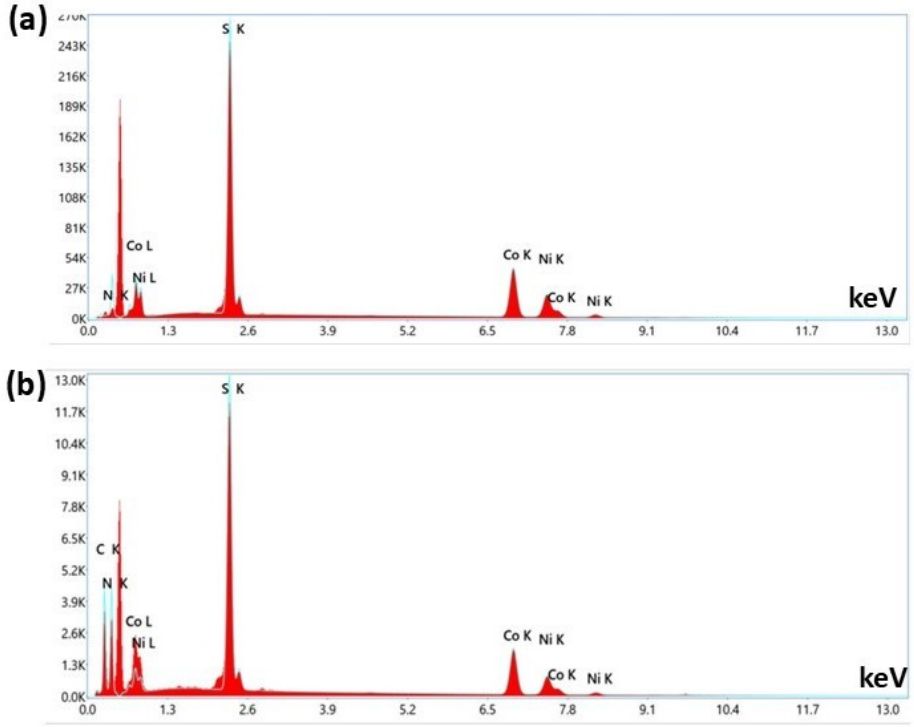

Fig.S1: Elemental composition (a) S'N-NCS and (b) S'N-NCS -S-g-CN.

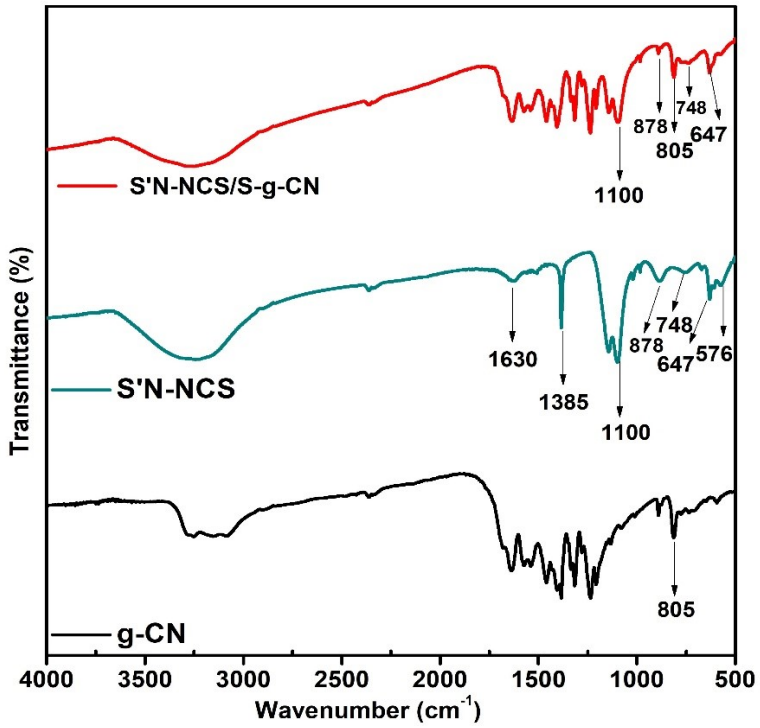

Figure S2. represents FTIR spectra of g-CN, S'N-NCS and S'N-NCS/S-g-CN.

Figure S3 represents FTIR spectra of g-CN, S'N-NCS and S'N-NCS/S-g-CN nanocomposite. The formation of g-C_3N_4 is clearly observed through FTIR spectra and the peak located at 805 cm^{-1} could be due to the characteristics breathing mode of tri-s-triazine units. The peak appeared at around 1200-1650 can be typically assigned for breathing mode of CN heterocycles. [1] The broad band in the range 3000-3400 cm^{-1} can be ascribed to the stretching vibration of uncondensed amine group and surface adsorbed water molecule. For, S'N-NCS, the band appeared at 576, 647, 748 and 878 cm^{-1} are assigned for symmetrical stretching vibration of Co-S or Ni-S vibration of $NiCo_2S_4$. Moreover, an intense doublet peak at 1100 cm^{-1} is due to bending vibration of sulfide groups present in S'N-NCS. [2] The peak appeared at 1385 and 1630 cm^{-1} might be due to the presence of residual interlayer nitrite anions and bending vibrations of adsorbed water molecules.[3] In S'N-NCS/S-g-CN nanocomposite characteristics peaks observed for g-C_3N_4 and for S'N-NCS ($NiCO_2S_4$) confirming formation of S'N-NCS/S-g-CN nanocomposite.

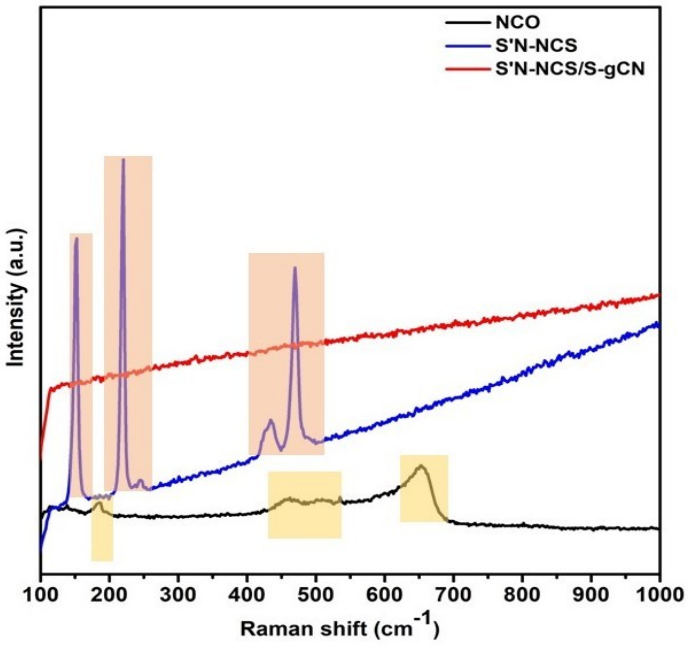

Figure S3. represents Raman spectra of NCO, S'N-NCS and S'N-NCS/S-g-CN.

To understand the crystal structure of the as prepared materials Raman spectroscopy has been carried out. Fig, S4 represent the Raman spectra of NCO, S'N-NCS and S'N-NCS/S-g-CN. For NCO, it shows peaks at 183, 463, 517, and 655 cm^{-1}, which are due to F2g, Eg, F2g and A1g mode of $NiCo_2O_4$. From the spectrum of NCO, the only band observed for Ni-O and Co-O, absence of other band confirming purity of $NiCo_2O_4$ (i.e NCO). [4] Spectrum for S'N-NCS ($NiCo_2S_4$) typically provide several prominent peaks. The peak appeared at around 150 cm^{-1} can be ascribed due to the asymmetric bending of (S-Ni_{tetra}-S) bonds. The bending of (S-Ni_{tetra}-S) causes Eg (218 and 240 cm^{-1}) mode which may arise due to torsional mode of M-S bond and sulfur ring vibration. The peak around 434 and 460 Cm^{-1} (Eg) might be due to breathing mode involving in-plane and out-plane vibration of sulfur atoms. The observed band confirmed formation of $NiCo_2S_4$. [5,6] In case of S'N-NCS/S-g-CN, a plateau like spectrum noticed and it might be because of presence of g-CN which has weak efficiency towards Raman scattering. As S'N-NCS/S-g-CN possesses a remarkable amount of g-CN, it might be one of the possible causes to get plateau like spectrum.

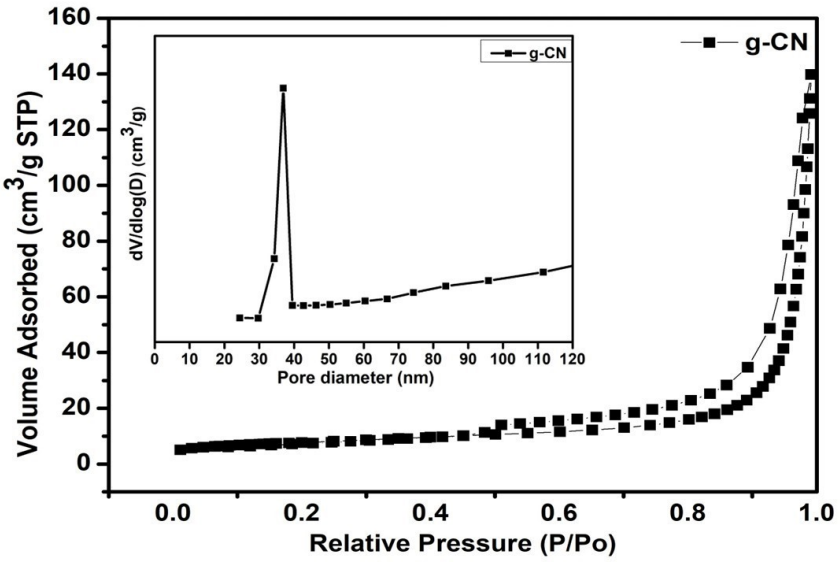

Figure S4: N_2 adsorption desorption isotherm of g-CN.

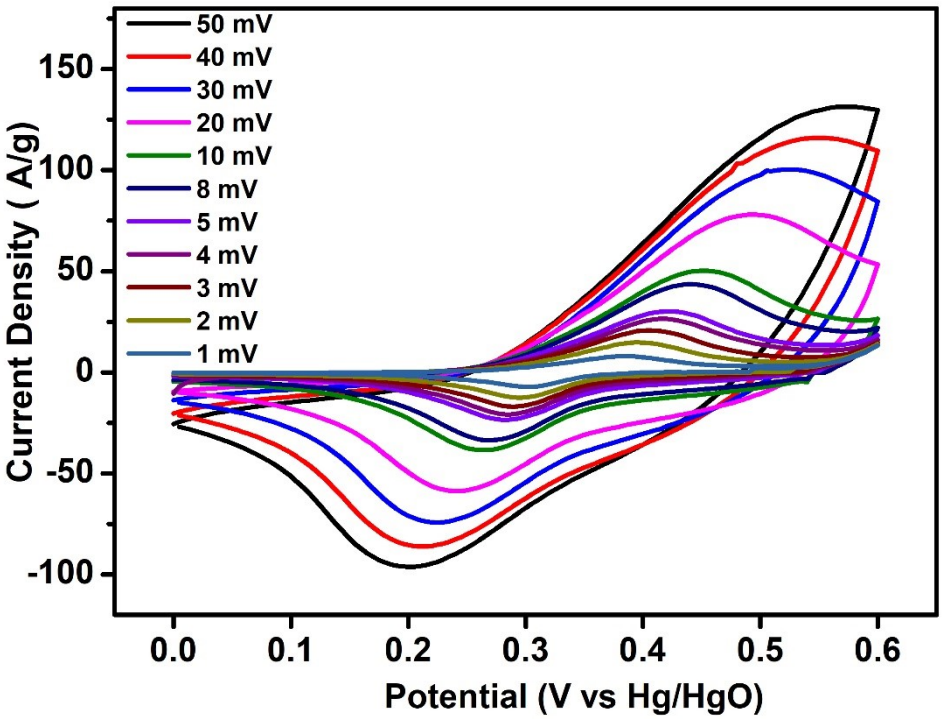

Figure S5 represents CV profile of S'N-NCS.

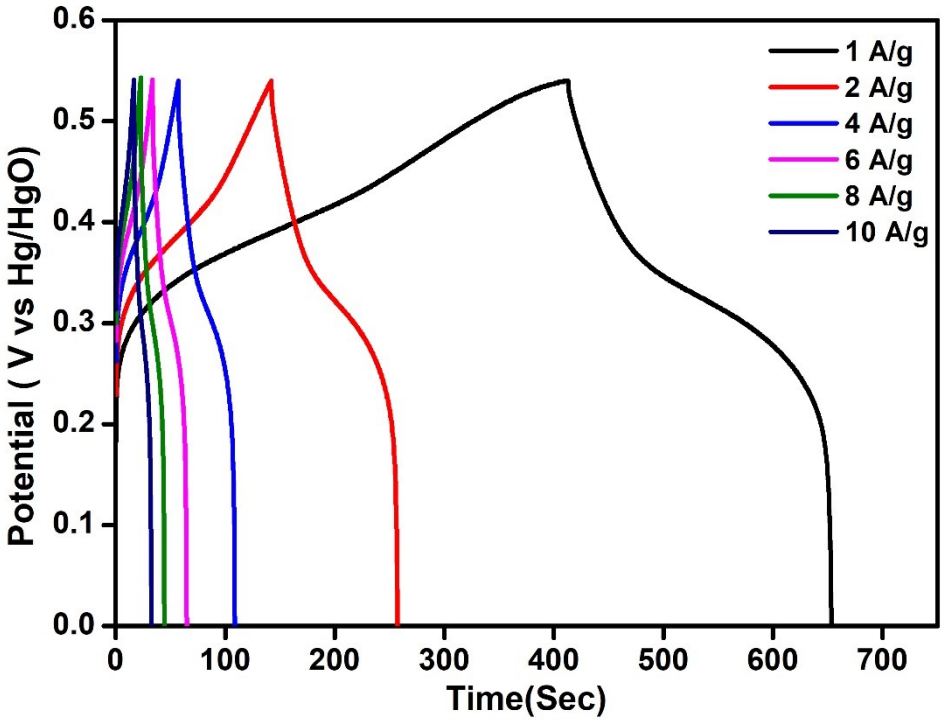

Figure S6 represents GCD profile of S'N-NCS.

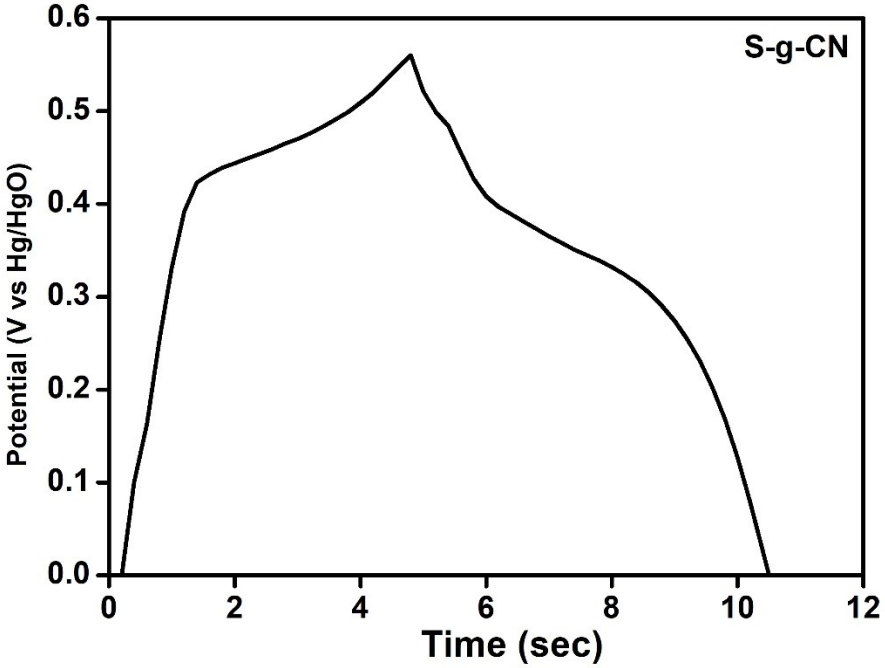

Figure S7 represents GCD profile of S-g-CN.

Table S1 represents the specific capacity of S'N-NCS, S-g-CN and S'N-NCS/S-g-CN at different current density.

Current Density (A/g)		**1**	**2**	**4**	**6**	**8**	**10**
Specific Capacity (C/g)	**S'N-NCS**	242	208	202	189	179	158
	S-g-CN	9	-	-	-	-	-
	S'N-NCS/S-g-CN	1034	972	904	827	766	732

Theoretical specific capacitance Calculation:

Theoretical capacitance has been calculated by using the following equation

$$C_t = \frac{n \times f}{\Delta V \times m}$$

Where

n = number of moles of electrons transmitted per mole of active material (n=4)

f= faraday constant (96485 C/mol)

m= molar mass of active material (g/mol) [$NiCo_2S_4$ =304.793 g/Mol]

ΔV= potential (0.5)

$$C_t = \frac{4 \times 96485}{0.5 \times 304.8} = 2532.4 \text{ F/g}$$

Table S2 Represents the comparison among the various $NiCo_2S_4$ based electrode materials with our work.

Materials	**Specific Capacitance (C/g or F/g)**	**Electrolyte**	**Ref.**
$NiCo_2S_4$@$NiMoO_4$	1035 F g^{-1} at 1 A g^{-1}	3 M KOH aqueous	7

		electrolyte.	
Hollow C-$NiCo_2S_4$	1722 F g^{-1} / 688.8 C g^{-1} at 1 A g^{-1}	6 M KOH solution	8
Mesoporous $NiCo_2O_4$ and $NiCo_2S_4$	1296 F g^{-1} at a current density of 1 A g^{-1}	1 M KOH	9
Glycine-assisted hydrothermal synthesis of NiCo2S4	675 F g^{-1} at 1 A g^{-1}	6M KOH	10
$NiCo_2S_4$/S-doped g-C_3N_4	351.0 F g^{-1} at 1 A g^{-1}	2M KOH	11
$NiCo_2S_4$ nanosheets on porous g-C_3N_4 nanosheets	506 C g^{-1} at 1 A g^{-1}	2M KOH	12
Sulfur vacancy mediated N-$NiCo_2S_4$ /S-g-C_3N_4	1034 C g^{-1} at 1A g^{-1} in	2M KOH	Our work

Reference

(1) S. Pany and K. M. Parida, *Phys. Chem. Chem. Phys.,* 2015, **17**, 8070-8077.
(2) Malaya K. Sahoo and G. Ranga Rao, *Electrochimica Acta*, 2018, **268**, 139-149.
(3) S. Pany, K. M. Parida, and B. Naik, *RSC Adv.* 2013, **3,** 4976-4984.
(4) M. Silambarasan, P. S. Ramesh and D. Geetha, *J Mater Sci: Mater Electron*, 2017, **28**, 323-336.
(5) A. Premkumar, B. Sridevi and K. S. Mohan, J. Appl. Electrochem., DOI: 10.1007/s10800-024-02170-4.
(6) C. Xia, P. Li, A. N. Gandi, U. Schwingenschlogl and H. N. Alshareef, Chem. Mater. 2015, 27, 6482-6485.
(7) J.Wang, Y.Li, Y. Zhao, D. Zhang, S. Song and J. Ke, *Crystals*. 2022; ***12***, 821.
(8) S.G. Mohamed, I. Hussain and J.J. Shim, *Nanoscale*, 2018**, 10***,* 6620-6628.
(9) Y. Liu, Z. Wang, Y. Zhong, M. Tade, W. Zhou, Z. Shao, *Adv. Funct. Mater.* 2017, **27**, 1701229.
(10) M.S. Kumar, N. Bhagavath, S.K. Batabyal, N.K. Kothurkar*, JS: AMD*. 2019**, 4**, 376-380.

(11) J.S Ma, H. Yang, S. Kubendhirana , L.Y. Lin, *J. Alloys Compd*. 2022, **903**,163972.
(12) Z. Li, L.Wu, L. Wanga, A. Gua, Q. Zhou, *Electrochim Acta,* 2017, **231**,617-625.